

Implication of the existence of $J^{PC} = 0^{--} \bar{D}_s DK$ bound state on nature of $D_{s0}^*(2317)$ and new configuration of exotic state

Tian-Wei Wu,^{1,*} Ming-Zhu Liu,^{2,3,†} and Li-Sheng Geng^{4,5,6,7,8,‡}

¹*School of Science, Shenzhen Campus of Sun Yat-sen University, Shenzhen 518107, China*

²*Frontiers Science Center for Rare isotopes, Lanzhou University, Lanzhou 730000, China*

³*School of Nuclear Science and Technology, Lanzhou University, Lanzhou 730000, China*

⁴*School of Physics, Beihang University, Beijing 102206, China*

⁵*Sino-French Carbon Neutrality Research Center, École Centrale de Pékin/School of General Engineering, Beihang University, Beijing 100191, China*

⁶*Peng Huanwu Collaborative Center for Research and Education, Beihang University, Beijing 100191, China*

⁷*Beijing Key Laboratory of Advanced Nuclear Materials and Physics, Beihang University, Beijing 102206, China*

⁸*Southern Center for Nuclear-Science Theory (SCNT), Institute of Modern Physics, Chinese Academy of Sciences, Huizhou 516000, Guangdong Province, China*

(■Dated: January 22, 2025)

The discovery of numerous new hadrons in the last two decades provides an unprecedented opportunity to explore the non-perturbative QCD and hadron structure. Many of these hadrons cannot be understood as conventional $q\bar{q}$ mesons and qqq baryons but instead as hadronic molecules. The most essential ingredient in the hadronic molecule picture is the hadron-hadron interactions. Therefore, It is vital to calculate/verify the underlying hadron interactions both theoretically and experimentally. In this letter, utilizing the model-independent DK potential extracted from the relevant experimental data, we predict an exotic $J^{PC} = 0^{--} \bar{D}_s DK$ three-body hadronic molecule with a mass of 4310_{-24}^{+14} MeV. This state is exotic in two ways. First, the quantum number of $J^{PC} = 0^{--}$ cannot be formed by conventional $c\bar{c}$ mesons. Second, it cannot be a two-body state $\bar{D}_s D_{s0}^*$ because their interaction is weak rather robust. We further demonstrate that the $B^+ \rightarrow D^{*-} D^+ K^+$ decay could be a suitable channel for searching for the predicted exotic state.

Introduction.— Quantum chromodynamics (QCD), the fundamental theory of the strong interaction, displays strong couplings at low energies, leading to color confinement, i.e., the degrees of freedom are hadrons instead of quarks and gluons, which makes the study of the low-energy strong interactions difficult at the quark level. As a result, hadron spectroscopy is essential for studying the non-perturbative strong interactions, especially for the many new heavy hadrons observed since 2003. A remarkable feature of the spectrum of these heavy hadrons is that most are near the threshold of a pair of hadrons. The recent studies from the unquenched quark model [1–4], effective field theories [5–10], and lattice QCD [11–15] indicate that the heavy hadrons have strong couplings to a pair of hadrons, where the hadron-hadron interactions characterize the non-perturbative strong interaction. Such non-perturbative effects also appear in the final-state interactions of heavy hadron decays [16, 17] and their productions [18–20]. Therefore, the hadron-hadron interactions are crucial for understanding the properties of heavy hadrons.

A salient example is the DK interaction, whose study is experiencing a renaissance since the discovery of the $D_{s0}^*(2317)$ [21]. Assuming $D_{s0}^*(2317)$ as the $c\bar{s}$ charmed strange meson of $J^P = 0^+$, its mass is lower by around 160 MeV than the prediction of the Godfrey-Isgur model [22]. The mass puzzle of $D_{s0}^*(2317)$ is solved if the DK molecular component is embodied [2–4, 23–25]. With the scattering length and effective range of the DK scattering obtained in lattice QCD simulations [11, 14, 26], it is found that the DK molecular component accounts for more than 70% of the physical $D_{s0}^*(2317)$ wave function [2, 4, 6, 9, 10]. Due to the scarce experimental data for the $D_{s0}^*(2317)$, the verification of

the above picture from alternative physical observables is not realized yet. Studying the DK interaction and $D_{s0}^*(2317)$ in three-body hadron systems have been proposed [27], inspiring many studies on similar three-body hadronic molecules [27–34]. Three-body hadronic molecules are new configurations of hadron compositions and can further advance our understanding of hadronic matter and the non-perturbative strong interactions, which may also pave the way towards a new paradigm in the hadron spectroscopy.

Originally, the Valencia group employed the Fixed Center Approximation to the Faddeev equations and predicted the existence of two exotic hadrons: three-body NDK [35] and $DK\bar{K}$ [36] molecules, where the DK interaction is determined by reproducing the mass of $D_{s0}^*(2317)$. However, verifying the DK interaction via the above three-body hadron systems is less optimal since the DN and $K\bar{K}$ potentials are strongly attractive [35, 36]. Then, we turned to the DDK system. Since the DD interaction is weak, the DK interaction plays a dominant role in forming the DDK molecule [30, 37, 38]. On the other hand, it isn't easy to produce the DDK molecule in e^+e^- collisions [39]. It could be produced in B_c decays [27] but faces the challenge of the low production rate of B_c mesons. Later, a $D\bar{D}K$ molecule was also predicted [40], but its yield in the inclusive process of e^+e^- collisions is lower than that of the two-body DK molecule by three orders of magnitude [41]. In addition, other components can mix with the three-body hadronic molecule [42]. As a result, a good three-body molecule candidate without possible mixing with other components and likely produced in experiments is still missing, whose existence can play a significant role in confirming the existence of

three-body hadronic molecules and verifying the underlying hadron-hadron interactions.

In this letter, we obtain a $J^{PC} = 0^{--} \bar{D}_s DK$ three-body molecule with a binding energy of about a few tens of MeV. Such a quantum number is exotic for $c\bar{c}$ mesons, indicating that it can not mix with conventional charmonium states [43]. Moreover, the subsystem $J^{PC} = 0^{--} D_{s0}^* \bar{D}_s$ is hard to bind [44, 45], but the three-body system $\bar{D}_s DK$ can bind, indicating this three-body molecule can not mix with two-body molecules. In addition, such a $\bar{D}_s DK$ molecule can be produced in B decays. The observation by the LHCb Collaboration is promising, considering its decay behaviors and production rates.

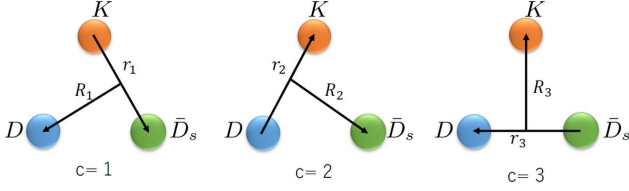


FIG. 1. Three permutations of the Jacobi coordinates for the $\bar{D}_s DK$ system.

Theoretical framework.— We first construct a three-body wave function for the $\bar{D}_s DK$ system of good C parity:

$$\Psi^C = \frac{1}{\sqrt{2}}(\Psi_{\bar{D}_s DK} + C\Psi'_{D_s \bar{D}K}), \quad (1)$$

where the eigenvalue $C = \pm 1$ and Ψ (Ψ') is the wave func-

tion of $\bar{D}_s DK$ ($D_s \bar{D}K$) system. The wave function Ψ^C can be solved by Schrödinger equation with the Hamiltonian $H = T + T' + V + V' + V^C$, where T (T') and V (V') are the kinetic energy term and the hadron-hadron potentials of Ψ (Ψ'), respectively. The potential V^C dependent on the C -parity could be a three-body interaction and correlate the wave function Ψ and Ψ' . Here, since the DK potential can form a bound state D_{s0}^* , we use the two-body $\bar{D}_s D_{s0}^*$ potential.

With the potentials, the Schrödinger equation of Ψ^C can be simplified as

$$\langle \Psi^C | (T + V + CV_{\bar{D}_s D_{s0}^* - D_s \bar{D}K}^C - E) | \Psi^C \rangle = 0, \quad (2)$$

which can be solved by the Gaussian Expansion Method (GEM) with three Jacobi channels shown in Fig. 1 [46]. The details of the GEM calculations are introduced in the Supplemental Material.

As shown in the following, there exists a $J^{PC} = 0^{--} \bar{D}_s DK$ molecule (denote by X) in this work. Since the decays and productions of the X play an important role in its likely experimental discovery, we employ the triangle mechanism to study its partial decay and production in B decays [47, 48]. From the analysis of the weights of Jacobi configurations in Fig. 1, we assume that the X decays via the subsystem $\bar{D}_s D_{s0}^*$, which then inelastically scatters into $J/\psi\eta$, $\bar{D}^* D$, and $\bar{D}_s^* D_s$ via the meson exchange mechanism, as illustrated in Fig. 2. These Feynman diagrams can be calculated using the effective Lagrangian approach. The Lagrangians describing the interactions of each vertex in the triangle diagrams are shown in the Supplemental Material. With the Lagrangian for each vertex in Fig. 2, we obtain the corresponding amplitudes as

$$i\mathcal{M}_a = g_{XD_{s0}^* \bar{D}_s} g_{D_{s0}^* D_s \eta} g_{\psi \bar{D}_s D_s} \int \frac{d^4 q}{(2\pi)^4} (k_1^\mu - q^\mu) \frac{1}{k_1^2 - m_{D_{s0}^*}^2} \frac{1}{k_2^2 - m_{\bar{D}_s}^2} \frac{1}{q^2 - m_{D_s}^2} \varepsilon_\mu(p_2) F(q^2), \quad (3)$$

$$i\mathcal{M}_b = g_{XD_{s0}^* \bar{D}_s} g_{D_{s0}^* D_s \eta} g_{\bar{D}_s D_s^* \eta} \int \frac{d^4 q}{(2\pi)^4} q^\mu \frac{1}{k_1^2 - m_{D_{s0}^*}^2} \frac{1}{k_2^2 - m_{\bar{D}_s}^2} \frac{1}{q^2 - m_\eta^2} \varepsilon_\mu(p_2) F(q^2), \quad (4)$$

$$i\mathcal{M}_c = g_{XD_{s0}^* \bar{D}_s} g_{D_{s0}^* DK} g_{\bar{D}_s D^* K} \int \frac{d^4 q}{(2\pi)^4} q^\mu \frac{1}{k_1^2 - m_{D_{s0}^*}^2} \frac{1}{k_2^2 - m_{\bar{D}_s}^2} \frac{1}{q^2 - m_K^2} \varepsilon_\mu(p_2) F(q^2), \quad (5)$$

where the molecule couplings to their constituents are determined by the residues of the pole obtained by solving the Lippmann-Schwinger equation [49], i.e., $g_{XD_{s0}^* \bar{D}_s} = 15.86 \pm 2.34$ GeV, $g_{D_{s0}^* DK} = 11.39 \pm 1.17$ GeV, and $g_{D_{s0}^* D_s \eta} = 7.51 \pm 1.11$ GeV. Moreover, the other couplings are determined as $g_{\psi \bar{D}_s D_s} = 5.8 \pm 0.9$, $g_{D_s D_s^* \eta} = 5.72 \pm 0.58$, and $g_{D_s D^* K} = 14.00 \pm 1.73$ via SU(3)-flavor symmetry [50].

Since the minimum quark constituent of the X is $c\bar{c}$, it will likely be observed in B decays. It is well known that many charmonium/charmoniumlike states are produced in B decays, proceeding via the decay $b \rightarrow c\bar{c}s$ at the

quark level [27, 51]. However, such decay modes are color-suppressed and can not be factorized in the naive factorization approach. The final-state interaction is an effective approach to deal with the non-perturbative effect in heavy-hadron weak decays [47, 52–57].

In this letter, we assume that the B meson firstly decays into a pair of \bar{D}^* and D_{s0}^* mesons, and then the \bar{D}^* meson scatters into \bar{D}_s and K mesons. Finally, the $\bar{D}_s DK$ molecule is dynamically generated by the subsystem $\bar{D}_s D_{s0}^*$ as shown in Fig. 3. In Ref. [49, 58], the productions of D_{s0}^* as a hadronic molecule in B decays are investigated, which laid the four-

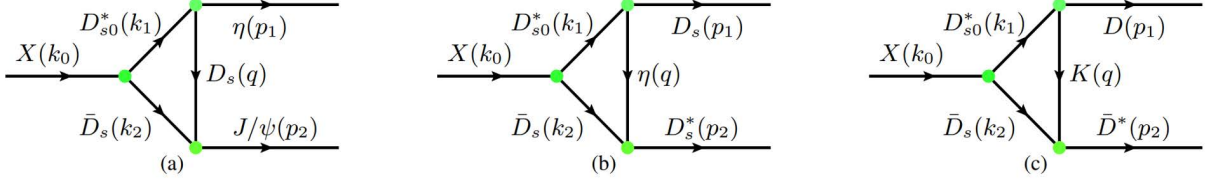


FIG. 2. Triangle diagrams of the X via the subsystem $D_{s0}^* \bar{D}_s$ decaying into $J/\psi \eta$, $D_s \bar{D}_s^*$, and $D \bar{D}^*$.

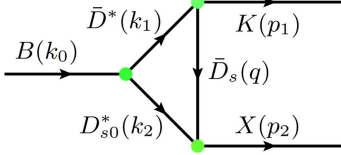


FIG. 3. Triangle diagrams accounting for the weak decays of $B \rightarrow XK$.

dition for the present study. Similarly, we employ the effective Lagrangian approach to calculate the Feynman diagram of Fig. 3, and its amplitude is written as

$$\mathcal{M} = g_{\bar{D}^* \bar{D}_s K} g_{D_{s0}^* \bar{D}_s X} \mathcal{A}(B \rightarrow D_{s0}^* \bar{D}^*)^\mu \quad (6)$$

$$\frac{-g^{\mu\nu} + \frac{k_1^\mu k_1^\nu}{k_1^2}}{(k_1^2 - m_{\bar{D}^*}^2)(k_2^2 - m_{\bar{D}_s}^2)(q^2 - m_{\bar{D}_s}^2)} p_1^\nu F(q^2),$$

where the amplitude $\mathcal{A}(B \rightarrow D_{s0}^* \bar{D}^*)$ is shown in the Supplemental Material. To avoid the ultraviolet divergence of the above loop integral and account for the internal structure of the involved hadrons, we add the following form factor in the meson exchange vertex,

$$F(q, \Lambda, m) = \left(\frac{\Lambda^2 - m_E^2}{\Lambda^2 - q^2} \right)^2, \quad (7)$$

where m_E represents the mass of the exchanged particle and Λ is an unknown parameter, which can be further parameterized as $\Lambda = \alpha \Lambda_{QCD} + m_E$ [47, 59].

The partial decay widths of Fig. 2 and Fig. 3 can be finally obtained as

$$\Gamma = \frac{1}{2J+1} \frac{1}{8\pi} \frac{|\vec{p}|}{M^2} |\bar{\mathcal{M}}|^2, \quad (8)$$

where J is the total angular momentum of the initial state M , the overline indicates the sum over the polarization vectors of final states, and $|\vec{p}|$ is the momentum of either final state in the rest frame of M .

Results and discussions.— In this letter, we employ the contact-range effective field theory (EFT) to construct the DK , $\bar{D}_s K$, and $D \bar{D}_s$ potentials [49, 60]. Since the $D_{s0}^* \bar{D}_s$ potential associated with the C -parity of the $\bar{D}_s DK$ system can not be determined by the contact-range EFT, we employ the one boson exchange (OBE) model [45, 61]. By reproducing the masses of the exotic states as well as using the

TABLE I. Binding energy (in units of MeV) and weights of Jacobi channels of $0^{- -}$ $\bar{D}_s DK$ molecule based on the components of the $D_{s0}^*(2317)$.

Sets	B.E.($0^{- -}$)	$P_{\bar{D}_s K - D}$	$P_{DK - \bar{D}_s}$	$P_{\bar{D}_s D - K}$
$\alpha = 1$	22_{-14}^{+23}	$11_{-1}^{+1} \%$	$78_{+2}^{-1} \%$	$11_{-1}^{+0} \%$
$\alpha = 2$	20_{-13}^{+22}	$10_{-1}^{+1} \%$	$80_{+2}^{-1} \%$	$10_{-1}^{+0} \%$

SU(3)-flavor symmetry [11, 62–65], we found that the DK , $\bar{D}_s K$, and $D \bar{D}_s$ contact potentials satisfy approximately the following relationship: $C_a^{DK} : C_a^{\bar{D}_s K} : C_a^{D \bar{D}_s} = 1 : 0.5 : 0.1$ for a cutoff of $\Lambda = 1$ GeV. Since the DK potential plays an important role, we show below the detail of determining the DK interaction by reproducing the mass of $D_{s0}^*(2317)$.

To precisely determine the DK interaction, we assume the $D_{s0}^*(2317)$ as a mixture of a $DK - D_s \eta$ molecular state and a $c\bar{s}$ bare state rather than a pure DK molecule. The lattice QCD simulations or reanalysis of lattice QCD results [2, 4, 6, 9–11, 14, 26] found that the molecular component accounts for more than 70% of the $D_{s0}^*(2317)$ wave function. Therefore, we assume that the molecular and bare components account for 70% and 30% of the physical $D_{s0}^*(2317)$. In the mixture picture, the extracted DK potential forms a bound state with a binding energy of 14 MeV, which is less attractive than assuming $D_{s0}^*(2317)$ as a pure DK molecule. To estimate the uncertainty of the extracted DK potential, we vary the molecular compositeness of $D_{s0}^*(2317)$ from 50% to 100%, and then similarly determine the DK interaction as shown in Table II of the Supplemental Material.

With the so-obtained potentials, the $\bar{D}_s DK$ system is calculated with GEM. To be consistent with the meson exchange mechanism in Fig. 2 and Fig. 3, we vary the α of the $\bar{D}_s D_{s0}^* \rightarrow D_s \bar{D}_s^*$ OBE potential from 1 to 2. Two bound states with $J^{PC} = 0^{- -}$ and $0^{- +}$ are generated, and the latter is more bound than the former, where the binding energies are weakly dependent on α . The results for the $J^{PC} = 0^{- +}$ state are listed in the Supplemental Material. As shown in Table I, the binding energy of the $0^{- -}$ $\bar{D}_s DK$ bound state is about 21_{-14}^{+24} MeV. Our results indicate that, as the $DK - D_s \eta$ molecular component of the $D_{s0}^*(2317)$ is in the range of 50% \sim 100%, the $\bar{D}_s DK$ system always remains bound. Interestingly, the weights of Jacobi channels $c = 1 - 3$ in Fig. 1 are stable, which are about 10%, 80%, and 10% of $\bar{D}_s K - D$, $DK - \bar{D}_s$ and $\bar{D}_s D - K$, respectively, varying only 1 \sim 2 percent. This indicates the $0^{- -}$ three-body bound state is mainly

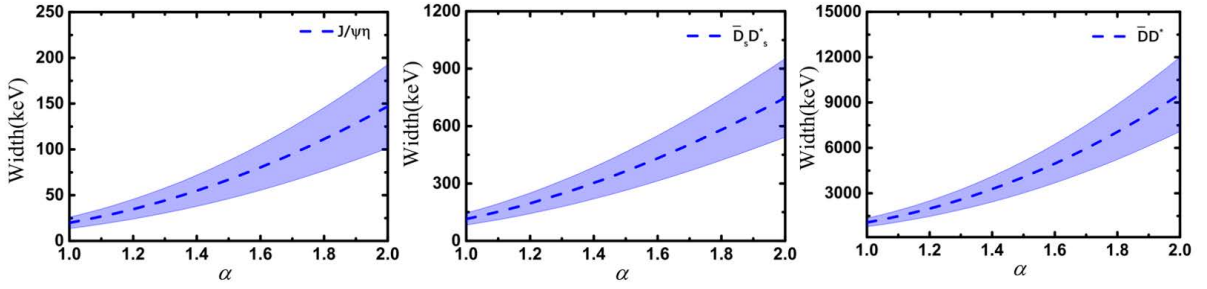


FIG. 4. Partial decay widths of $X \rightarrow J/\psi\eta$, $X \rightarrow \bar{D}_s D_s^*$, and $X \rightarrow \bar{D}^* D$ as functions of α . The dashed line and band correspond to their central value and uncertainties.

composed of the $(DK) - \bar{D}_s$ channel, weakly dependent on the molecular component of the $D_{s0}^*(2317)$. To test the impact of cutoff to our results, the mass of X as a function of the cutoff R_c is shown in Fig. 5, which indicates that its mass is weakly dependent on the cutoff.

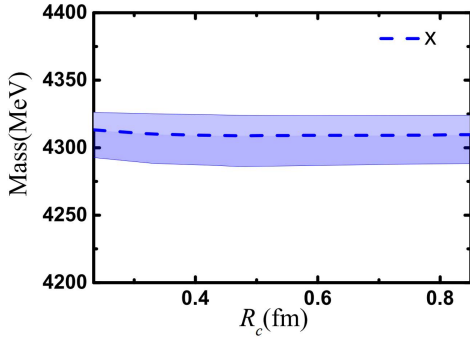


FIG. 5. Mass of X as a function of the cutoff R_c .

Next, we turn to the strong decays and production of X . In our study, in addition to the parameter α uncertainties, the dominant uncertainties originate from the couplings of the three vertices of the triangle diagrams. As a result, we obtain the uncertainties of the decay widths originating from the uncertainties of these parameters via a Monte Carlo sampling in their 1σ intervals.

From our analysis, the X decays into $J/\psi\eta$, $D_s \bar{D}_s^*$, and $D \bar{D}^*$. Its mass is estimated to be 4310_{-24}^{+14} MeV. In Fig. 4, we show the partial decay widths of $X = 4310$ MeV as a function of α , where the uncertainties of the couplings of vertices induce the bands. We can see that the partial widths of the decays $X \rightarrow J/\psi\eta$, $X \rightarrow \bar{D}_s D_s^*$, and $X \rightarrow \bar{D}^* D$ are up to the order of 10^1 , 10^2 , and 10^3 keV, indicating that the partial decay width of $X \rightarrow \bar{D}^* D$ is larger than those of $X \rightarrow \bar{D}_s D_s^*$ and $X \rightarrow J/\psi\eta$ by one and two orders of magnitude, respectively. In Fig. 1 of the Supplemental Material, we show the partial decay widths of $X = 4286$ MeV and $X = 4324$ MeV. The ratio of $\Gamma(X \rightarrow \bar{D}^* D)/\Gamma(X \rightarrow \bar{D}_s D_s^*)$ lies in the range of $9.9 \sim 13.6$, $9.3 \sim 12.6$, and $8.7 \sim 11.8$ for the lower, center, and upper mass of X , and the corresponding ratio of $\Gamma(X \rightarrow \bar{D}_s D_s^*)/\Gamma(X \rightarrow J/\psi\eta)$ lies in the range of $5.2 \sim 6.1$, $5.1 \sim 5.7$, and $4.9 \sim 5.4$. Regardless of

the mass of X , the ratio of $\Gamma(X \rightarrow \bar{D}^* D) : \Gamma(X \rightarrow \bar{D}_s D_s^*) : \Gamma(X \rightarrow J/\psi\eta) \approx 50 : 5 : 1$. Therefore, we conclude that the $J^{PC} = 0^{--} \bar{D}_s DK$ molecule dominantly decays into $\bar{D}^* D$.

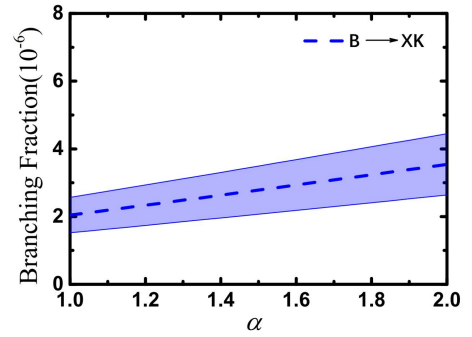


FIG. 6. Branching fraction of the decays $B \rightarrow KX$ as a function of α .

Finally, we analyze the production rate of X in B decays. In Fig. 6, we show the branching fraction of the decay $B \rightarrow KX$ as a function of α , where $X = 4310$ MeV. One can see that the branching fraction of the decay $B \rightarrow KX$ is up to the order of 10^{-6} . Moreover, as shown in Fig. 2 of the Supplemental Material, the production rate of X in B decays is still of the order of 10^{-6} for its lower and upper mass. Thus, the production rate of the $J^{PC} = 0^{--} \bar{D}_s DK$ molecule in B decays is up to the order of 10^{-6} . Comparing with the yields of $D_{s0}^*(2317)$ in B decays [49], we find that the production rate of the two-body molecule DK in B decays is larger than that of three-body molecule $\bar{D}_s DK$ in B decay by three orders of magnitude, consistent with the ratio of the yields of the two-body molecule DK to that of the three-body molecule $\bar{D} \bar{D} K$ in e^+e^- collisions [41], indicating that the ratio of the production rates of the DK molecule to those of the $D \bar{D}_{(s)} K$ molecule is only dependent on the long-range interaction but independent on the short-range interaction in the production process.

Our results indicate that the X dominantly decays into $\bar{D}^* D$. In the isospin limit, the branching fraction of X decays into $\bar{D}^{*0} D^0$, $\bar{D}^0 D^{*0}$, $D^{*+} D^-$, and $D^+ D^{*-}$ is around 0.25. As a result, we estimate the branching fraction of the decay $B^+ \rightarrow (X \rightarrow D^{*-} D^+) K^+$ up to be 5×10^{-7} . Re-

ferring to the branching fraction $\mathcal{B}(B^+ \rightarrow D^{*-}D^+K^+) = 6 \times 10^{-4}$ [66, 67], we estimate the ratio of $\mathcal{B}[B^+ \rightarrow (X \rightarrow D^{*-}D^+)K^+]/\mathcal{B}(B^+ \rightarrow D^{*-}D^+K^+) \sim 10^{-3}$. The event number of the decay $B^+ \rightarrow D^{*-}D^+K^+$ of the LHCb Collaboration corresponding to an integrated luminosity of 9 fb^{-1} is around 2×10^3 [68]. We can expect that the event number of the decay $B^+ \rightarrow (X \rightarrow D^{*-}D^+)K^+$ would reach up to be at least 10 and 10^2 corresponding to the integrated luminosity of 50 fb^{-1} and 350 fb^{-1} .

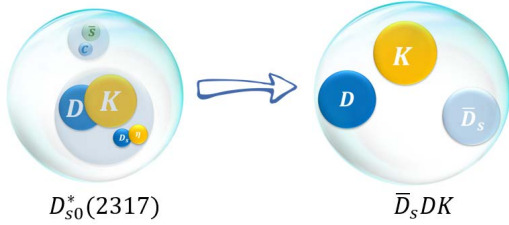


FIG. 7. With the DK potential determined by reproducing the mass of the $D_{s0}^*(2317)$ as a mixture of a $DK - D_s\eta$ molecular state and a $c\bar{s}$ bare state, a three-body $\bar{D}_s DK$ molecule is predicted.

Summary and outlook.— Some exotic states discovered in the past 20 years are widely regarded as hadronic molecular candidates, which not only motivate us to study the hadron-hadron interaction but also offer the opportunity to investigate the existence of three-body hadronic molecules. In this letter, with the DK interaction determined by the $D_{s0}^*(2317)$ assuming as a mixture state, we predicted a rather special three-body hadronic molecule $J^{PC} = 0^{--} \bar{D}_s DK$ with a mass of about 4310 MeV as shown in Fig. 7. A careful study of its decay behaviors and production mechanism shows that it dominantly decays into \bar{D}^*D , and its production rate in B decays is of the order of 10^{-6} . In particular, we found that the ratio of the production rates of the DK molecule to those of the $D\bar{D}_{(s)}K$ molecules is only dependent on the long-range interaction of the production processes, indicating that the formation of three-body hadronic molecules is responsible by the non-perturbative strong interaction.

Moreover, the event number of the decay $B^+ \rightarrow (X \rightarrow D^{*-}D^+)K^+$ in the LHC corresponding to the integrated luminosity of 50 fb^{-1} and 350 fb^{-1} is estimated to be at least 10 and 10^2 , respectively. It should be noted that the LHCb Collaboration observed the signal of $J^{PC} = 0^{--}$ charmonium/charmoniumlike states in the decay $B^+ \rightarrow D^{*-}D^+K^+$ [68]. Therefore, the observation of the $J^{PC} = 0^{--} \bar{D}_s DK$ molecule by the LHCb Collaboration in the future is promising. On the other hand, the $0^{--} \bar{D}_s DK$ three-body bound state is easily distinguished from charmonium states and two-body molecules. The discovery of the $0^{--} \bar{D}_s DK$ three-body hadronic molecule will extend the configuration of the hadron spectrum and help derive the hadron-hadron interaction even pinpoint the molecular nature of $D_{s0}^*(2317)$. We strongly recommend experimental searches for the $0^{--} \bar{D}_s DK$ molecule in the decay channel $B^+ \rightarrow \bar{D}^{*0}D^0K^+$.

Acknowledgement.— This work is partly supported by the National Key R&D Program of China under Grant No. 2023YFA1606703 and the National Natural Science Foundation of China under Grant No. 12435007. Tian-Wei Wu acknowledges support from the National Natural Science Foundation of China under Grant No.12405108. Ming-Zhu Liu acknowledges support from the National Natural Science Foundation of China under Grant No.12105007.

* wutw6@mail.sysu.edu.cn

† Corresponding author: liumz@lzu.edu.cn

‡ Corresponding author: lisheng.geng@buaa.edu.cn

- [1] P. G. Ortega, J. Segovia, D. R. Entem, and F. Fernandez, Phys. Rev. D **94**, 074037 (2016), arXiv:1603.07000 [hep-ph].
- [2] M. Albaladejo, P. Fernandez-Soler, J. Nieves, and P. G. Ortega, Eur. Phys. J. C **78**, 722 (2018), arXiv:1805.07104 [hep-ph].
- [3] S.-Q. Luo, B. Chen, X. Liu, and T. Matsuki, Phys. Rev. D **103**, 074027 (2021), arXiv:2102.00679 [hep-ph].
- [4] Z. Yang, G.-J. Wang, J.-J. Wu, M. Oka, and S.-L. Zhu, Phys. Rev. Lett. **128**, 112001 (2022), arXiv:2107.04860 [hep-ph].
- [5] H.-Y. Cheng and F.-S. Yu, Phys. Rev. D **89**, 114017 (2014), arXiv:1404.3771 [hep-ph].
- [6] A. Martínez Torres, E. Oset, S. Prelovsek, and A. Ramos, JHEP **05**, 153 (2015), arXiv:1412.1706 [hep-lat].
- [7] Z.-H. Guo, U.-G. Meißner, and D.-L. Yao, Phys. Rev. D **92**, 094008 (2015), arXiv:1507.03123 [hep-ph].
- [8] D.-L. Yao, M.-L. Du, F.-K. Guo, and U.-G. Meißner, JHEP **11**, 058 (2015), arXiv:1502.05981 [hep-ph].
- [9] F.-K. Guo, PoS LATTICE2022, 232 (2023).
- [10] F. Gil-Domínguez and R. Molina, Phys. Rev. D **109**, 096002 (2024), arXiv:2306.01848 [hep-ph].
- [11] L. Liu, K. Orginos, F.-K. Guo, C. Hanhart, and U.-G. Meißner, Phys. Rev. D **87**, 014508 (2013), arXiv:1208.4535 [hep-lat].
- [12] D. Mohler, C. B. Lang, L. Leskovec, S. Prelovsek, and R. M. Woloshyn, Phys. Rev. Lett. **111**, 222001 (2013), arXiv:1308.3175 [hep-lat].
- [13] C. B. Lang, L. Leskovec, D. Mohler, S. Prelovsek, and R. M. Woloshyn, Phys. Rev. D **90**, 034510 (2014), arXiv:1403.8103 [hep-lat].
- [14] G. S. Bali, S. Collins, A. Cox, and A. Schäfer, Phys. Rev. D **96**, 074501 (2017), arXiv:1706.01247 [hep-lat].
- [15] C. Alexandrou, J. Berlin, J. Finkenrath, T. Leontiou, and M. Wagner, Phys. Rev. D **101**, 034502 (2020), arXiv:1911.08435 [hep-lat].
- [16] X.-Y. Guo, Y. Heo, and M. F. M. Lutz, Phys. Rev. D **98**, 014510 (2018), arXiv:1801.10122 [hep-lat].
- [17] H.-L. Fu, H. W. Griethammer, F.-K. Guo, C. Hanhart, and U.-G. Meißner, Eur. Phys. J. A **58**, 70 (2022), arXiv:2111.09481 [hep-ph].
- [18] F. S. Navarra, M. Nielsen, E. Oset, and T. Sekihara, Phys. Rev. D **92**, 014031 (2015), arXiv:1501.03422 [hep-ph].
- [19] M. Albaladejo, D. Jido, J. Nieves, and E. Oset, Eur. Phys. J. C **76**, 300 (2016), arXiv:1604.01193 [hep-ph].
- [20] M.-Z. Liu, X.-Z. Ling, L.-S. Geng, En-Wang, and J.-J. Xie, Phys. Rev. D **106**, 114011 (2022), arXiv:2209.01103 [hep-ph].
- [21] B. Aubert et al. (BaBar), Phys. Rev. Lett. **90**, 242001 (2003), arXiv:hep-ex/0304021.
- [22] S. Godfrey and N. Isgur, Phys. Rev. D **32**, 189 (1985).
- [23] W. Hao, Y. Lu, and B.-S. Zou, Phys. Rev. D **106**, 074014

- (2022), arXiv:2208.10915 [hep-ph].
- [24] J.-J. Yang, W. Hao, X. Wang, D.-M. Li, Y.-X. Li, and E. Wang, *Eur. Phys. J. C* **83**, 1098 (2023), arXiv:2303.11815 [hep-ph].
- [25] R.-H. Ni, J.-J. Wu, and X.-H. Zhong, *Phys. Rev. D* **109**, 116006 (2024), arXiv:2312.04765 [hep-ph].
- [26] G. K. C. Cheung, C. E. Thomas, D. J. Wilson, G. Moir, M. Pardon, and S. M. Ryan (Hadron Spectrum), *JHEP* **02**, 100 (2021), arXiv:2008.06432 [hep-lat].
- [27] M.-Z. Liu, Y.-W. Pan, Z.-W. Liu, T.-W. Wu, J.-X. Lu, and L.-S. Geng, *Phys. Rept.* **1108**, 1 (2025), arXiv:2404.06399 [hep-ph].
- [28] A. Martinez Torres, K. P. Khemchandani, D. Gamermann, and E. Oset, *Phys. Rev. D* **80**, 094012 (2009), arXiv:0906.5333 [nucl-th].
- [29] L. Ma, Q. Wang, and U.-G. Meißner, *Chin. Phys. C* **43**, 014102 (2019), arXiv:1711.06143 [hep-ph].
- [30] T.-W. Wu, M.-Z. Liu, L.-S. Geng, E. Hiyama, and M. P. Valderrama, *Phys. Rev. D* **100**, 034029 (2019), arXiv:1906.11995 [hep-ph].
- [31] A. Martinez Torres, K. P. Khemchandani, L. Roca, and E. Oset, *Few Body Syst.* **61**, 35 (2020), arXiv:2005.14357 [nucl-th].
- [32] X. Wei, Q.-H. Shen, and J.-J. Xie, *Eur. Phys. J. C* **82**, 718 (2022), arXiv:2205.12526 [hep-ph].
- [33] Y. Tan, X. Liu, X. Chen, Y. Yang, H. Huang, and J. Ping, *Phys. Rev. D* **110**, 016005 (2024), arXiv:2404.02048 [hep-ph].
- [34] Z. Zhang, X.-Y. Hu, G. He, J. Liu, J.-A. Shi, B.-N. Lu, and Q. Wang, (2024), arXiv:2409.01325 [hep-ph].
- [35] C. W. Xiao, M. Bayar, and E. Oset, *Phys. Rev. D* **84**, 034037 (2011), arXiv:1106.0459 [hep-ph].
- [36] V. R. Debastiani, J. M. Dias, and E. Oset, *Phys. Rev. D* **96**, 016014 (2017), arXiv:1705.09257 [hep-ph].
- [37] A. Martinez Torres, K. P. Khemchandani, and L.-S. Geng, *Phys. Rev. D* **99**, 076017 (2019), arXiv:1809.01059 [hep-ph].
- [38] J.-Y. Pang, J.-J. Wu, and L.-S. Geng, *Phys. Rev. D* **102**, 114515 (2020), arXiv:2008.13014 [hep-lat].
- [39] Y. Li et al. (Belle), *Phys. Rev. D* **102**, 112001 (2020), arXiv:2008.13341 [hep-ex].
- [40] T.-W. Wu, M.-Z. Liu, and L.-S. Geng, *Phys. Rev. D* **103**, L031501 (2021), arXiv:2012.01134 [hep-ph].
- [41] T.-C. Wu and L.-S. Geng, *Phys. Rev. D* **108**, 014015 (2023), arXiv:2211.01846 [hep-ph].
- [42] M. Sanchez Sanchez, L.-S. Geng, J.-X. Lu, T. Hyodo, and M. P. Valderrama, *Phys. Rev. D* **98**, 054001 (2018), arXiv:1707.03802 [hep-ph].
- [43] T. Ji, X.-K. Dong, F.-K. Guo, and B.-S. Zou, *Phys. Rev. Lett.* **129**, 102002 (2022), arXiv:2205.10994 [hep-ph].
- [44] M. Karliner and J. L. Rosner, *Nucl. Phys. A* **954**, 365 (2016), arXiv:1601.00565 [hep-ph].
- [45] L.-L. Shen, X.-L. Chen, Z.-G. Luo, P.-Z. Huang, S.-L. Zhu, P.-F. Yu, and X. Liu, *Eur. Phys. J. C* **70**, 183 (2010), arXiv:1005.0994 [hep-ph].
- [46] E. Hiyama, Y. Kino, and M. Kamimura, *Prog. Part. Nucl. Phys.* **51**, 223 (2003).
- [47] H.-Y. Cheng, C.-K. Chua, and A. Soni, *Phys. Rev. D* **71**, 014030 (2005), arXiv:hep-ph/0409317.
- [48] A. Faessler, T. Gutsche, V. E. Lyubovitskij, and Y.-L. Ma, *Phys. Rev. D* **76**, 014005 (2007), arXiv:0705.0254 [hep-ph].
- [49] M.-Z. Liu, X.-Z. Ling, and L.-S. Geng, *Phys. Rev. D* **109**, 056014 (2024), arXiv:2312.01433 [hep-ph].
- [50] M. E. Bracco, M. Chiapparini, F. S. Navarra, and M. Nielsen, *Prog. Part. Nucl. Phys.* **67**, 1019 (2012), arXiv:1104.2864 [hep-ph].
- [51] H.-X. Chen, *Phys. Rev. D* **105**, 094003 (2022), arXiv:2103.08586 [hep-ph].
- [52] X.-Q. Li and B.-S. Zou, *Phys. Lett. B* **399**, 297 (1997), arXiv:hep-ph/9611223.
- [53] D.-S. Du, X.-Q. Li, Z.-T. Wei, and B.-S. Zou, *Eur. Phys. J. A* **4**, 91 (1999), arXiv:hep-ph/9805260.
- [54] Y.-S. Dai, D.-S. Du, X.-Q. Li, Z.-T. Wei, and B.-S. Zou, *Phys. Rev. D* **60**, 014014 (1999), arXiv:hep-ph/9903204.
- [55] M. Ablikim, D.-S. Du, and M.-Z. Yang, *Phys. Lett. B* **536**, 34 (2002), arXiv:hep-ph/0201168.
- [56] C.-D. Lu, Y.-L. Shen, and W. Wang, *Phys. Rev. D* **73**, 034005 (2006), arXiv:hep-ph/0511255.
- [57] Y. Cao, Y. Cheng, and Q. Zhao, *Phys. Rev. D* **109**, 073002 (2024), arXiv:2303.00535 [hep-ph].
- [58] A. Faessler, T. Gutsche, S. Kovalenko, and V. E. Lyubovitskij, *Phys. Rev. D* **76**, 014003 (2007), arXiv:0705.0892 [hep-ph].
- [59] M.-Z. Liu, J.-J. Xie, and L.-S. Geng, *Phys. Rev. D* **102**, 091502 (2020), arXiv:2008.07389 [hep-ph].
- [60] C. Hidalgo-Duque, J. Nieves, and M. P. Valderrama, *Phys. Rev. D* **87**, 076006 (2013), arXiv:1210.5431 [hep-ph].
- [61] X. Liu, Z.-G. Luo, and S.-L. Zhu, *Phys. Lett. B* **699**, 341 (2011), [Erratum: *Phys. Lett. B* **707**, 577 (2012)], arXiv:1011.1045 [hep-ph].
- [62] F.-K. Guo, P.-N. Shen, H.-C. Chiang, R.-G. Ping, and B.-S. Zou, *Phys. Lett. B* **641**, 278 (2006), arXiv:hep-ph/0603072 [hep-ph].
- [63] F.-K. Guo, C. Hanhart, and U.-G. Meissner, *Eur. Phys. J. A* **40**, 171 (2009), arXiv:0901.1597 [hep-ph].
- [64] M. Altenbuchinger, L. S. Geng, and W. Weise, *Phys. Rev. D* **89**, 014026 (2014), arXiv:1309.4743 [hep-ph].
- [65] T. Ji, X.-K. Dong, M. Albaladejo, M.-L. Du, F.-K. Guo, J. Nieves, and B.-S. Zou, (2022), 10.1016/j.scib.2023.02.034, arXiv:2212.00631 [hep-ph].
- [66] P. del Amo Sanchez et al. (BaBar), *Phys. Rev. D* **83**, 032004 (2011), arXiv:1011.3929 [hep-ex].
- [67] R. Aaij et al. (LHCb), *JHEP* **12**, 139 (2020), arXiv:2005.10264 [hep-ex].
- [68] R. Aaij et al. (LHCb), *Phys. Rev. Lett.* **133**, 131902 (2024), arXiv:2406.03156 [hep-ex].
- [69] M.-Z. Liu, F.-Z. Peng, M. Sánchez Sánchez, and M. P. Valderrama, *Phys. Rev. D* **98**, 114030 (2018), arXiv:1811.03992 [hep-ph].
- [70] F.-Z. Peng, M.-Z. Liu, M. Sánchez Sánchez, and M. Pavon Valderrama, *Phys. Rev. D* **102**, 114020 (2020), arXiv:2004.05658 [hep-ph].
- [71] Y.-s. Oh, T. Song, and S. H. Lee, *Phys. Rev. C* **63**, 034901 (2001), arXiv:nucl-th/0010064.
- [72] R. C. Verma, *J. Phys. G* **39**, 025005 (2012), arXiv:1103.2973 [hep-ph].
- [73] Q. Wu, M.-Z. Liu, and L.-S. Geng, *Eur. Phys. J. C* **84**, 147 (2024), arXiv:2304.05269 [hep-ph].
- [74] N. Ikeno, G. Toledo, and E. Oset, *Phys. Lett. B* **847**, 138281 (2023), arXiv:2305.16431 [hep-ph].
- [75] P.-P. Shi, M. Albaladejo, M.-L. Du, F.-K. Guo, and J. Nieves, (2024), arXiv:2410.19563 [hep-ph].
- [76] B. Aubert et al. (BaBar), *Phys. Rev. Lett.* **93**, 041801 (2004), arXiv:hep-ex/0402025.
- [77] T. Iwashita et al. (Belle), *PTEP* **2014**, 043C01 (2014), arXiv:1310.2704 [hep-ex].
- [78] R. Aaij et al. (LHCb), *JHEP* **04**, 046 (2022), arXiv:2202.04045 [hep-ex].
- [79] S. Navas et al. (Particle Data Group), *Phys. Rev. D* **110**, 030001 (2024).

SUPPLEMENTAL MATERIAL

In this Supplemental Material, we provide some details about how to solve the $\bar{D}_s DK$ three-body system with GEM and relevant hadron-hadron interactions and how the Feynman diagrams of Fig. 2 and Fig. 3 in the main manuscript are calculated in the effective Lagrangian approach. In addition, we present the contact-range EFT in which the $D_{s0}^*(2317)$ is dynamically generated in three scenarios, and the partial decay widths and the production rate of X in B decays.

GEM TO SOLVE THE $\bar{D}_s DK$ THREE-BODY SYSTEM

TABLE I. Quantum numbers of the Jacobi coordinate channels ($c = 1 - 3$) of the $\bar{D}_s DK$ three-body systems.

c	l	L	λ	t	T	s	S	J	P	C	n_{max}	N_{max}
1	0	0	0	$\frac{1}{2}$	0	0	0	0	-	-(+)	10	10
2	0	0	0	0	0	0	0	0	-	-(+)	10	10
3	0	0	0	$\frac{1}{2}$	0	0	0	0	-	-(+)	10	10

We use GEM to solve the following Schrödinger equation in Eq.(2) to study the $\bar{D}_s DK$ system

$$\langle \Psi | (T + V + CV_{\bar{D}_s D_{s0}^* - D_s \bar{D}_{s0}^*}^C - E) | \Psi \rangle = 0. \quad (9)$$

The spatial wave function of each channel has the following form

$$\Psi = \sum_{c=1}^3 \Phi_{\alpha}^c(\mathbf{r}_c, \mathbf{R}_c), \quad (10)$$

where α is a set of quantum numbers labeling the wave function. The quantum numbers of all the allowed configurations are determined by angular momentum conservation, isospin conservation, parity conservation, and C -parity conservation. Given that only S -wave interactions are considered, we have $l = L = \lambda = J = 0$. Since D_s is isospinless and only the DK interaction in $I = 0$ is dominant, the total isospin of these systems should be 0. The used configurations are shown in Table I.

The spatial wave function $\Phi_{lL,\lambda}^c$ is given in terms of Gaussian basis functions

$$\Phi_{lL,\lambda}^c(\mathbf{r}_c, \mathbf{R}_c) = [\phi_{ncl_c}^G(\mathbf{r}_c) \psi_{NcLc}^G(\mathbf{R}_c)]_{\lambda}, \quad (11)$$

$$\phi_{nlm}^G(\mathbf{r}_c) = N_{nl} r_c^l e^{-\nu_n r_c^2} Y_{lm}(\hat{r}_c), \quad (12)$$

$$\psi_{NLM}^G(\mathbf{R}_c) = N_{NL} R_c^L e^{-\lambda_n R_c^2} Y_{LM}(\hat{R}_c). \quad (13)$$

Here $N_{nl}(N_{NL})$ are the normalization constants of the Gaussian basis and the range parameters ν_n and λ_n are given by

$$\begin{aligned} \nu_n &= 1/r_n^2, & r_n &= r_{min} a^{n-1} \quad (n = 1, n_{max}), \\ \lambda_N &= 1/R_N^2, & R_N &= R_{min} A^{N-1} \quad (N = 1, N_{max}), \end{aligned} \quad (14)$$

in which $\{n_{max}, r_{min}, a \text{ or } r_{max}\}$ and $\{N_{max}, R_{min}, A \text{ or } R_{max}\}$ are Gaussian basis parameters.

The kinetic energy term corresponds to Jacobi channel c reads

$$T = -\frac{\hbar^2}{2m} \nabla_{r_c}^2 - \frac{\hbar^2}{2M} \nabla_{R_c}^2 \quad (15)$$

where m and M are the reduced masses corresponding to the coordinates r and R . The potential includes two parts, the two-body C -parity independent potentials $V = V_{\bar{D}_s K}(r_1) + V_{DK}(r_2) + V_{\bar{D}_s D}(r_3)$ and the C -parity dependent potential $V_{\bar{D}_s D_{s0}^* - D_s \bar{D}_{s0}^*}^C(R_2)$, which are introduced in the hadron-hadron potentials section.

After the basis expansion, the Schrödinger equation of this system is transformed into a generalized matrix eigenvalue problem:

$$\sum [T_{\alpha\alpha'}^{ab} + V_{\alpha\alpha'}^{ab} - EN_{\alpha\alpha'}^{ab}] C_{b,\alpha'} = 0. \quad (16)$$

Here, $T_{\alpha\alpha'}^{ab} = \langle \Phi_{\alpha}^a | T | \Phi_{\alpha'}^b \rangle$ is the kinetic matrix element, $V_{\alpha\alpha'}^{ab} = \langle \Phi_{\alpha}^a | V + CV_{\bar{D}_s D_{s0}^* - D_s \bar{D}_{s0}^*}^C | \Phi_{\alpha'}^b \rangle$ is the potential matrix element and $N_{\alpha\alpha'}^{ab} = \langle \Phi_{\alpha}^a | \Phi_{\alpha'}^b \rangle$ is the normalization matrix element. The eigenenergy E and coefficients are determined by the Rayleigh-Ritz variational principle. Thus, the binding energies and spatial structures can be studied.

HADRON-HADRON POTENTIALS

TABLE II. Masses of $DK - D_s\eta$ and DK molecules (in units of MeV), and probabilities in $D_{s0}^*(2317)$ based on the different molecular components of $D_{s0}^*(2317)$.

Components of $D_{s0}^*(2317)$	$M(DK - D_s\eta)$	$M(DK)$	$M(c\bar{s})$ [4]	$P(c\bar{s})$	$P(DK)$	$P(D_s\eta)$
70% molecule+30% $c\bar{s}$	2280	2349	2406	30%	60%	10%
100% molecule	2318	2358	2406	0%	90%	10%
50% molecule+50% $c\bar{s}$	2230	2336	2406	50%	42%	8%

In this letter, we employ the contact-range EFT to construct the hadron-hadron interaction. The DK , $\bar{D}_s K$, and $D\bar{D}_s$ potentials in momentum space are characterized by an unknown parameter C_a [49, 60]. Since the three-body Schrödinger equation is solved in coordinate space, the above contact-range potentials are transformed into $C_a\delta^3(\vec{r})$ [69]. The $\delta^3(\vec{r})$ term can be regulated by a Gaussian shape regulator so that the contact-range potential can be transferred into a finite-range one

$$V(r) = C_a \frac{e^{-(r/R_c)^2}}{\pi^{3/2} R_c^3}, \quad (17)$$

where R_c is a cut-off radius of the order of a typical hadronic size.

For DK interaction, we use the $D_{s0}^*(2317)$ as the input. In this letter, the $D_{s0}^*(2317)$ is regarded as a mixture of a $DK - D_s\eta$ molecular state and a $c\bar{s}$ bare state, in which the former accounts for about 70% and the later accounts for 30%. In terms of the relativistic quark model [4], the mass of $0^+ c\bar{s}$ bare state is adopted to be 2406 MeV [4]. The coupled-channel $DK - D_s\eta$ contact potential is written as [49]

$$V_{DK-D_s\eta}^{J^P=0^+} = \begin{pmatrix} V_{DK}(r) & -\frac{\sqrt{3}}{2}V_{DK}(r) \\ -\frac{\sqrt{3}}{2}V_{DK}(r) & 0 \end{pmatrix}. \quad (18)$$

The strength C_a of the DK interaction can be determined by the leading-order chiral perturbation theory [30], i.e., the Weinberg-Tomozawa term $C_a^{DK} = -\frac{C_W}{2f_\pi^2}$, where $C_W = 2$ and $f_\pi = 130$ MeV [11], resulting in the value of $C_a^{DK} = -2.24$ fm². Assuming the $D_{s0}^*(2317)$ as a mixture of a $DK - D_s\eta$ molecule and a $c\bar{s}$ bare state, R_c is determined as 0.472 fm. As indicated in Ref. [69], the result of $R_c = 0.5$ fm in coordinate space is equal to the result of $\Lambda = 1$ GeV in momentum space. The DK potential determined for $R_c = 0.472$ fm should be consistent with that for $\Lambda = 1$ GeV. As shown later, the DK potential in the third scenario is determined as $C_a^{DK} = -2.06$ fm², consistent with that in coordinate space. With such a DK potential, we found a bound state with a binding energy of 14 MeV, which indicates that the obtained DK potential is less attractive than that of assuming D_{s0}^* as a pure DK bound state, consistent with the conclusion derived in momentum space. In addition, we make the molecule compositeness of $D_{s0}^*(2317)$ range from 50% to 100% to estimate the uncertainties of the input. Accordingly, we can obtain the corresponding DK interaction, of which R_c ranges from 0.4383 – 0.513 fm. The results are summarized in Table II. Once the DK potential is determined, the $\bar{D}_s K$ potential is determined as half of the DK potential from the SU(3)-flavor symmetry, i.e., $V_{\bar{D}_s K}(r) = \frac{1}{2}V_{DK}(r)$ [11, 62–64].

For the $\bar{D}_s D$ interaction, we use $X(3872)$ as the input. $X(3872)$ can be regarded as a $1^{++} \bar{D}^* D$ bound state. By fitting $X(3872)$ with the contact-range EFT, the strength of the $\bar{D}^* D$ potential $C_a^{\bar{D}^* D}$ is about -0.79 fm² and $R_c = 0.434$ fm. According to the light meson saturation approach [70], we have $C_a^{\bar{D}^* D} : C_a^{\bar{D}_s D} = 1.35 : 0.42$, resulting $C_a = -0.24$ fm².

Since no experiment inputs can determine the $\bar{D}_s D_{s0}^*$ contact-range potential, we turn to the OBE model for help. In Refs. [45, 61], the authors claimed that the η and ϕ meson exchange are responsible for $\bar{D}_s D_{s0}^* \rightarrow D_s \bar{D}_{s0}^*$ potential, where the latter meson generates attractive interaction, but the former is attractive and repulsive for the charge parity $C = +$ and $C = -$, respectively. Therefore, the potential of $J^{PC} = 0^{-+} \bar{D}_s D_{s0}^*$ is more attractive than that of $J^{PC} = 0^{--} \bar{D}_s D_{s0}^*$, consistent with Ref. [44]. As for the three-body system, only the term on the C -parity is adopted. The one η exchange potential for the $\bar{D}_s D_{s0}^*$ system is written as

$$V_{\bar{D}_s D_{s0}^* - D_s \bar{D}_{s0}^*}^C = -\frac{2}{3} \frac{k^2}{f_\pi^2} q_0^2 Y(r, m_{eff}, \Lambda), \quad (19)$$

where $q_0 = m_{D_{s0}^*} - m_{D_s}$, $k = 0.56$, $f_\pi = 130$ MeV [61], and $\Lambda = \alpha \Lambda_{QCD} + m_{eff}$, $m_{eff} = \sqrt{m_\eta^2 - (m_{D_{s0}^*} - m_{D_s})^2}$.

TABLE III. $D_{s0}^*(2317)$ coupling to its constituents (in units of GeV).

Couplings	$X = 4.286$	$X = 4.310$	$X = 4.324$
$g_{XD_{s0}^*\bar{D}_s}$	21.72 ± 4.28	15.86 ± 2.34	9.86 ± 0.81
$g_{D_{s0}^*DK}$	14.61 ± 2.03	11.39 ± 1.17	7.79 ± 1.08
$g_{D_{s0}^*D_s\eta}$	9.47 ± 1.65	7.51 ± 1.11	4.93 ± 0.27

EFFECTIVE LAGRANGIANS

The Lagrangians describing the interactions between the hadronic molecules and their constituents are written as

$$\begin{aligned}\mathcal{L}_{XD_{s0}^*\bar{D}_s} &= g_{XD_{s0}^*\bar{D}_s} XD_{s0}^* \bar{D}_s, \\ \mathcal{L}_{D_{s0}^*D_s\eta} &= g_{D_{s0}^*D_s\eta} D_{s0}^* D_s \eta, \\ \mathcal{L}_{D_{s0}^*DK} &= g_{D_{s0}^*DK} D_{s0}^* DK,\end{aligned}\quad (20)$$

where g with different subscript denote the bound-state coupling to their constituents. In this letter, we take the mass of X under the $DK\bar{D}_s$ mass threshold 21_{-14}^{+24} MeV, where the $D_{s0}^*\bar{D}_s$ sub-system account for around 80% of the total wave function. Therefore, the couplings of $g_{XD_{s0}^*\bar{D}_s}$, $g_{D_{s0}^*D_s\eta}$, and $g_{D_{s0}^*DK}$ are estimated by the contact-range EFT as shown in Table III, where the uncertainties of the couplings come from the cutoff varying from 1 to 2 GeV. It should be noted that the D_{s0}^* is not the $D_{s0}^*(2317)$ instead of a DK bound state with a binding energy of 21_{-14}^{+24} MeV.

The Lagrangian describing the charmed mesons couplings to one light meson and J/ψ are written as [71]

$$\begin{aligned}\mathcal{L}_{\psi\bar{D}_sD_s} &= ig_{\psi\bar{D}_sD_s} \psi_\mu (\partial^\mu D_s \bar{D}_s^\dagger - D_s \partial^\mu \bar{D}_s^\dagger), \\ \mathcal{L}_{D_sD_s^*\eta} &= -ig_{D_sD_s^*\eta} (D_s \partial^\mu \eta D_{s\mu}^{*\dagger} - D_{s\mu}^* \partial^\mu \eta D_s^\dagger), \\ \mathcal{L}_{D_sD^*K} &= -ig_{D_sD^*K} (D_s \partial^\mu K D_\mu^{*\dagger} - D_\mu^* \partial^\mu K D_s^\dagger).\end{aligned}\quad (21)$$

The amplitude of the weak decay $B(k_0) \rightarrow D_{s0}^*(q_1) \bar{D}^*(q_2)$, described by the naive factorization approach [49], is written as

$$\begin{aligned}\mathcal{A}(B \rightarrow D_{s0}^* \bar{D}^*) &= \frac{G_F}{\sqrt{2}} V_{cb} V_{cs} a_1 f_{D_{s0}^*} \{-q_1 \cdot \varepsilon(q_2) (m_{D^*} + m_B) A_1(q_1^2) + (k_0 + q_2) \cdot \varepsilon(q_2) q_1 \cdot (k_0 + q_2) \\ &\quad \frac{A_2(q_1^2)}{m_{D^*} + m_B} + (k_0 + q_2) \cdot \varepsilon(q_2) [(m_{D^*} + m_B) A_1(q_1^2) - (m_B - m_{D^*}) A_2(q_1^2) - 2m_{D^*} A_0(q_1^2)]\},\end{aligned}\quad (22)$$

where $G_F = 1.166 \times 10^{-5}$ GeV⁻², $V_{cb} = 0.0395$, $V_{cs} = 0.991$, $f_{D_{s0}^*} = 59$ MeV, and $a_1 = 1.07$. The form factors of $A_0(t)$, $A_1(t)$, and $A_2(t)$ with $t \equiv q_1^2$ can be parameterized as [72]

$$X(t) = \frac{X(0)}{1 - a(t/m_B^2) + b(t^2/m_B^4)}.\quad (23)$$

For these form factors, we adopt those of the covariant light-front quark model, i.e., $(A_0(0), a, b)^{B \rightarrow \bar{D}^*} = (0.68, 1.21, 0.36)$, $(A_1(0), a, b)^{B \rightarrow \bar{D}^*} = (0.65, 0.60, 0.00)$, and $(A_2(0), a, b)^{B \rightarrow \bar{D}^*} = (0.61, 1.12, 0.31)$ [72]. Following Ref. [73], the $B \rightarrow \bar{D}^*$ transition results in a 10% uncertainty.

CONTACT-RANGE EFT

The following briefly introduces the contact-range EFT approach. The scattering amplitude T is responsible for the dynamical generations of hadronic molecules, which is obtained by solving the following Lippmann-Schwinger equation

$$T(\sqrt{s}) = (1 - VG(\sqrt{s}))^{-1}V,\quad (24)$$

where V is the hadron-hadron potential determined by the contact-range EFT approach, and $G(\sqrt{s})$ is the loop function of the two-body propagator. The loop functions of $G(\sqrt{s})$ is

$$G(s) = \int \frac{d^3q}{(2\pi)^3} \frac{e^{-2q^2/\Lambda^2}}{\sqrt{s} - m_1 - m_2 - q^2/(2\mu_{12}) + i\varepsilon},\quad (25)$$

where \sqrt{s} is the total energy in the center-of-mass frame of m_1 and m_2 , $\mu_{12} = \frac{m_1 m_2}{m_1 + m_2}$ is the reduced mass, and Λ is the momentum cutoff.

With the potentials, we can search for poles generated by the hadron-hadron interactions and determine the couplings between the molecular states and their constituents from the residues of the corresponding poles,

$$g_i g_j = \lim_{\sqrt{s} \rightarrow \sqrt{s_0}} (\sqrt{s} - \sqrt{s_0}) T_{ij}(\sqrt{s}), \quad (26)$$

where g_i denotes the coupling of channel i to the dynamically generated state and $\sqrt{s_0}$ is the pole position. With the couplings g_i , one can further obtain the compositeness of each component

$$P_i = -g_i^2 \frac{\partial G_{ii}(\sqrt{s})}{\partial \sqrt{s}}. \quad (27)$$

DK and $\bar{D}_s K$ potentials

TABLE IV. $D_{s_0}^*(2317)$ coupling to its constituents (in units of GeV).

Couplings	$\Lambda = 0.50$	$\Lambda = 1.00$	$\Lambda = 1.50$	$\Lambda = 2.00$	$\Lambda = 0.50$	$\Lambda = 1.00$	$\Lambda = 1.50$	$\Lambda = 2.00$
$g_{D_{s_0}^* DK}$	19.37	14.72	13.32	12.66	16.20	12.28	11.16	10.63
$g_{D_{s_0}^* D_s \eta}$	13.23	9.54	8.40	7.86	10.42	7.70	6.89	6.50
$C_a (\text{fm}^2)$	-5.78	-1.84	-1.03	-0.71	-6.96	-2.06	-1.12	-0.75
Compositeness	$\Lambda = 0.50$	$\Lambda = 1.00$	$\Lambda = 1.50$	$\Lambda = 2.00$	$\Lambda = 0.50$	$\Lambda = 1.00$	$\Lambda = 1.50$	$\Lambda = 2.00$
P_{DK}	0.92	0.90	0.89	0.88	0.65	0.63	0.62	0.62
$P_{D_s \eta}$	0.08	0.10	0.11	0.12	0.05	0.07	0.08	0.08

The *DK* contact-range interaction is parameterized by a constant C_a , and the *DK* – $D_s \eta$ coupled-channel contact-range potential V in matrix form read [49]

$$V_{DK-D_s \eta}^{JP=0^+} = \begin{pmatrix} C_a & -\frac{\sqrt{3}}{2} C_a \\ -\frac{\sqrt{3}}{2} C_a & 0 \end{pmatrix}. \quad (28)$$

To estimate the dressed effect of bare states, we have added an energy-dependent term

$$V = \alpha(s - \bar{s}), \quad (29)$$

where \bar{s} is the energy squared of the mass threshold. The unknown parameter α is determined by the weight of molecular components. Since recent studies showed that the molecular component account for more than 70% of the total wave function of $D_{s_0}^*(2317)$ [2, 19, 74], we set the weight as 70% to determine the value of α .

In the following, we study three scenarios to determine the *DK* interaction by reproducing the mass of $D_{s_0}^*(2317)$, i.e., the $D_{s_0}^*(2317)$ is assumed as a *DK* molecule, a $D_s \eta$ – *DK* molecule, and a mixture of 70% $D_s \eta$ – *DK* molecular component and 30% bare component. Assuming the $D_{s_0}^*(2317)$ as a *DK* bound state, one can determine the value of $C_a = -0.98 \text{ fm}^2$ for a cutoff $\Lambda = 2.0 \text{ GeV}$, $C_a = -1.41 \text{ fm}^2$ for a cutoff $\Lambda = 1.5 \text{ GeV}$, $C_a = -2.44 \text{ fm}^2$ for a cutoff $\Lambda = 1.0 \text{ GeV}$, and $C_a = -7.21 \text{ fm}^2$ for a cutoff $\Lambda = 0.5 \text{ GeV}$. Then, assuming that the $D_{s_0}^*(2317)$ is dynamically generated by *DK* and $D_s \eta$ coupled channels, one can determine the value of C_a as a function of cutoff in the left panel of Table IV. One can see that the size of C_a decreases, and the *DK* and $D_s \eta$ components account for around 90% and 10% of the total wave function, respectively. Finally, when taking into account the effect of bare states, we find that the size of C_a increases, a bit smaller than the first scenario. In the third scenario, the *DK* and $D_s \eta$ components account for around 63% and 7% of the total wave function. After the *DK* interaction is determined, the $\bar{D}_s K$ potential is determined as half of the *DK* potential from the SU(3)-flavor symmetry, i.e., $V_{\bar{D}_s K} = \frac{1}{2} V_{DK}$ [11, 62–64].

$\bar{D}_s D$ potential

For the scattering process $\bar{D}_s D \rightarrow \bar{D}_s D$, the contact potential is characterized by the parameter C_{1a} [60], which is the same as the isovector contact potential of $\bar{D} D \rightarrow \bar{D} D$ under SU(3)-flavor symmetry. In the following, we analyze the relationship

of parameters of contact-range EFT by the light meson saturation approach [70]. The contact-range potentials of the isoscalar $\bar{D}^{(*)}D^{(*)}$ system are parameterized as C_{0a} and C_{0b} , and the isovector $\bar{D}^{(*)}D^{(*)}$ system as C_{1a} and C_{1b} . According to the light meson saturation approach, we have the ratios $C_{0a} : C_{0b} : C_{1a} : C_{1b} = 1 : 0.35 : 0.42 : 0$. Identifying $X(3872)$ as the bound state of $J^{PC} = 1^{++}\bar{D}^*D$, one can obtain the sum of $C_{0a} + C_{0b} = -0.79 \text{ fm}^2$ for a cutoff $\Lambda = 1 \text{ GeV}$, then further obtain the values of $C_{0a} = -0.58 \text{ fm}^2$, $C_{0b} = -0.21 \text{ fm}^2$, and $C_{1a} = -0.24 \text{ fm}^2$. Similarly, we obtain the value of $C_{1a} = -0.60 \text{ fm}^2$ for a cutoff $\Lambda = 0.5 \text{ GeV}$, $C_{1a} = -0.15 \text{ fm}^2$ for a cutoff $\Lambda = 1.5 \text{ GeV}$, and $C_{1a} = -0.11 \text{ fm}^2$ for a cutoff $\Lambda = 2.0 \text{ GeV}$. In Ref. [65], Ji et al. obtained the value of $C_{1a} = -0.33 \pm 0.02 \text{ fm}^2$ for a cutoff $\Lambda = 1 \text{ GeV}$ by simulating the mass distributions of $\bar{D}_{(s)}D_{(s)}$ of the processes of $\gamma\gamma \rightarrow \bar{D}D$ and $B^+ \rightarrow K^+D_{(s)}^+D_{(s)}^-$, consistent with the analysis of the light meson saturation approach. A recent approach analyzing the Lattice QCD data of $\bar{D}D - \bar{D}_sD_s$ coupled-channel scattering, the value of C_{1a} is estimated to be in the range of $-0.44 \sim -0.64 \text{ fm}^2$ [75], a bit larger than our estimations and Ref. [65]. The ratio of the DK potential in the first scenario to the \bar{D}_sD potential is from 8.9 to 12.0, and the ratio of the DK potential in the third scenario to the \bar{D}_sD potential is from 6.8 to 11.6. The average of the above ratios is around 10.

ADDITIONAL RESULTS

Results of $J^{PC} = 0^{-+} \bar{D}_sDK$ molecule

TABLE V. Binding energy (in MeV) and weights of Jacobian channels of $0^{-+} \bar{D}_sDK$ based on the components of the $D_{s0}^*(2317)$.

Sets	B.E.(0^{-+})	$P_{\bar{D}_sK-D}$	$P_{DK-\bar{D}_s}$	$P_{\bar{D}_sD-K}$
$\alpha = 1$	26_{-16}^{+22}	$13_{-1}^{+0} \%$	$76_{+0}^{-0} \%$	$11_{+1}^{-0} \%$
$\alpha = 2$	28_{-17}^{+23}	$14_{-1}^{+0} \%$	$74_{+1}^{+1} \%$	$12_{+0}^{-1} \%$

The 0^{-+} state is a bit more bound than the 0^{-+} state due to the attractive interaction in positive C -parity, which is about $27_{-17}^{+24} \text{ MeV}$. The weights of Jacobi channels $c = 1 - 3$ are about 13%, 75% and 12% of $D_s\bar{K} - \bar{D}$, $\bar{D}\bar{K} - D_s$ and $D_s\bar{D} - \bar{K}$ respectively.

Results of strong decays and production rates

The main text only showed the partial decays and production rates for the mass $X = 4310 \text{ MeV}$. Here, we present the partial widths of the decays $X \rightarrow J/\psi\eta$, $X \rightarrow \bar{D}_sD_s^*$, and $X \rightarrow \bar{D}^*D$ as a function of α for the mass of $X = 4286 \text{ MeV}$ and $X = 4324 \text{ MeV}$, as shown in the up and down panels of Fig. 1. One can see that the absolute values of the partial decay width vary greatly, but their ratio varies little. Similarly, we present the production rates of the X in B decays for the mass of $X = 4286 \text{ MeV}$ and $X = 4324 \text{ MeV}$, as shown in the left and right panels of Fig. 2. We can see that the order of magnitude of the production rate is about 10^{-6} .

In addition, our results indicate that the branching fraction of the decay $X \rightarrow J/\psi\eta$ is up to the order of 10^{-2} , yielding the branching fraction $\mathcal{B}[B^+ \rightarrow (X \rightarrow J/\psi\eta)K^+] \sim 10^{-8}$. With the branching fraction $\mathcal{B}(B^+ \rightarrow J/\psi\eta K^+) = 10^{-4}$ [76, 77], we obtain the ratio $\mathcal{B}[B^+ \rightarrow (X \rightarrow J/\psi\eta)K^+]/\mathcal{B}(B^+ \rightarrow J/\psi\eta K^+) \sim 10^{-4}$. The LHCb Collaboration showed that the event number of the decay $B^+ \rightarrow J/\psi\eta K^+$ corresponding to an integrated luminosity of 9 fb^{-1} is around 5×10^3 [78], and its event number will reach up to 10 as the integrated luminosity of 350 fb^{-1} . As for the decay $B^+ \rightarrow (X \rightarrow D_s^{*+}D_s^-)K^+$, the D_s^{*+} meson dominantly decays into $D_s^+\gamma$, which would heavily reduce the detection efficiency in the LHCb detector. Additionally, the experimental branching fraction of the decay $B^+ \rightarrow D_s^{*+}D_s^-K^+$ is still missing [79]. Therefore, the most promising channel of observing the $J^{PC} = 0^{-+} \bar{D}_sDK$ molecule is $B^+ \rightarrow (X \rightarrow D^{*-}D^+)K^+$.

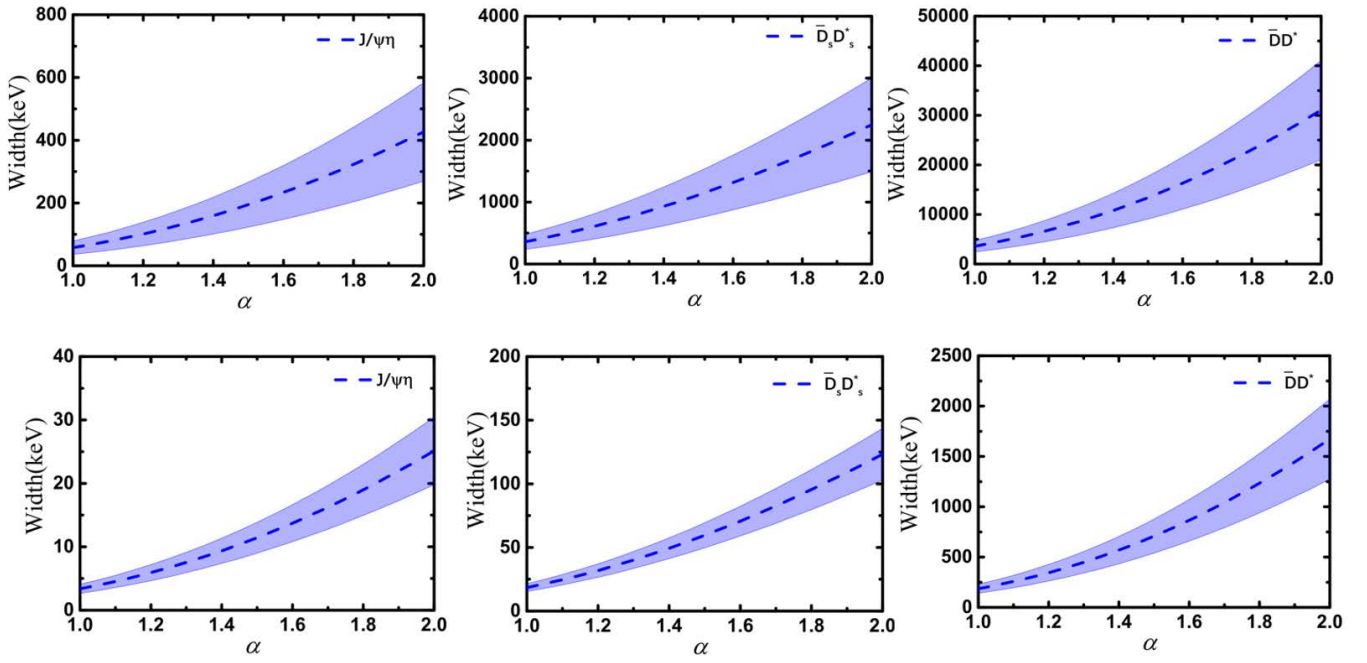


FIG. 1. Partial widths of the decays $X \rightarrow J/\psi\eta$, $X \rightarrow \bar{D}_s D_s^*$, and $X \rightarrow \bar{D}^* D$ as a function of α . The up and down panels correspond to the mass of $X = 4286$ MeV and $X = 4324$ MeV.

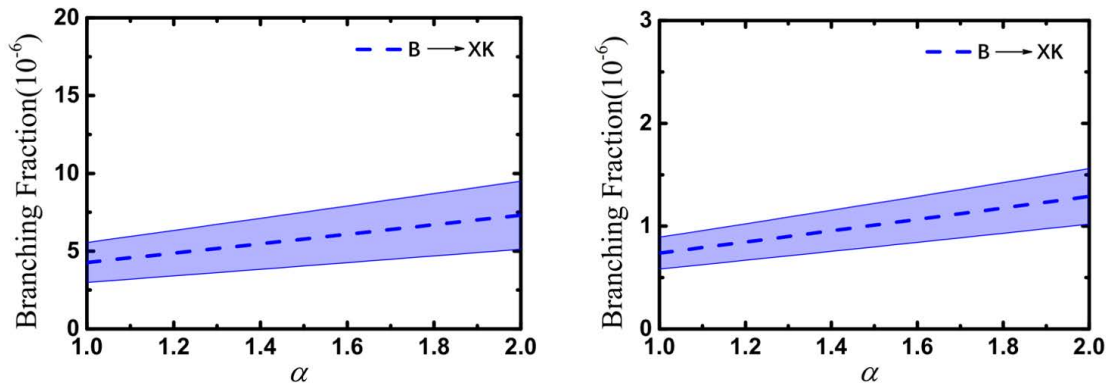


FIG. 2. Branching fraction of the decays $B \rightarrow KX$ as a function of α . The left and right panels correspond to the results for the mass of $X = 4286$ MeV and $X = 4324$ MeV.